Nuclear Engineering and Technology 54 (2022) 301–309

Contents lists available at ScienceDirect

Nuclear Engineering and Technology

journal homepage: www.elsevier.com/locate/net

Original article

Calculation of X-ray spectra characteristics and kerma to personal dose equivalent $H_p(10)$ conversion coefficients: Experimental approach and Monte Carlo modeling

A. Arectout [a, *], I. Zidouh [b], Y. Sadeq [d], M. Azougagh [c], B. Maroufi [e], E. Chakir [b], H. Boukhal [a]

[a] ERSN, Faculty of Sciences, Abdelmalek Essaadi University, Tetouan, Morocco
[b] LPMS, Faculty of Sciences, Ibn Tofail University, Kenitra, Morocco
[c] ENSAM Rabat, Mohammed V University, Morocco
[d] Centre National de radioprotection, salé, Morocco
[e] Faculty Ben M'sick, Hassan II University, Casablanca, Morocco

ARTICLE INFO

Article history:
Received 1 January 2021
Received in revised form
20 June 2021
Accepted 17 July 2021
Available online 22 July 2021

Keywords:
Radiation quality
X-ray
Conversion coefficient
Monte Carlo
GAMOS code

ABSTRACT

This work aims to establish some X-ray qualities recommended by the International Standard Organization (ISO) using the half-value layer (HVL) and $H_p(10)$ dosimetry approaches. The HVL values of the following qualities N-60, N-80, N-100, N-150 and N-250 were determined using various attenuation layers. The obtained results were compared to those of reference X-ray beam qualities and a good agreement was found (difference less than 5% for all qualities). The GAMOS (Geant4-based Architecture for Medicine-Oriented Simulations) radiation transport Monte Carlo toolkit was employed to simulate the production of X-ray spectra. The characteristics HVLs, mean energy and the spectral resolution of simulated spectra have been calculated and turned out to be conform to the ISO reference ones (difference less than the limit allowed by ISO). Furthermore, the conversion coefficients from air kerma to personal dose equivalent for simulated and measured spectra were fairly similar (the maximum difference less than 4.2%).

1. Introduction

Ionizing radiations are used in a wide variety of fields such as radiotherapy, industry, research, education, etc … Nevertheless this radiation can have harmful effects on human health. The radiation dose received by workers exposed to external ionizing radiation must be accurately determined in order to verify the conformity to the radiation protection requirements [1]. In order to achieve this, the dosimeters used to detect the radiation dose should be calibrated according to internationally recognized standards. The International Standard Organization defined, in the first part of the ISO-4037 standard, the methods for developing reference X-ray beam qualities for calibration purposes [2]. ISO defines the radiation qualities by their half-value layer (HVL), mean energy and spectral resolution. The X-ray spectra measurements have generally been performed using the spectrometry technique [3,4]. However, this technique is very expensive, time demanding and needs a proper correction of measured spectra by the detector response. Kurkova and Judas (2016) [4] show that the X-ray spectrometry technique faces two sorts of difficulties: the high photonuence rate and the spectrum distortion due to the random coincidences, escape effects, Compton effect … etc. In the recent years, a lot of research work have been carried out on the simulation of X-ray spectra using Monte Carlo simulation codes, such as MCNP4C [5], GEANT [6], FLUKA [7], PENELOPE [8] and EGSnrc [9] … etc. The spectra generated by these codes showed a good agreement as compared to the data available in the ISO standard.

Furthermore, the ISO 4037-2 standard [10] specifies another method to demonstrate that the X-ray spectral distribution is sufficiently close to that of a reference radiation field. This is done by means of $H_p(10)$ dosimetry approach. Since the instruments for radiation monitoring need to be calibrated in terms of a measurable quantity, conversion coefficients are calculated to relate some basic physical quantities like air kerma to the operational ones. The

* Corresponding author.
E-mail addresses: assiaarectout@gmail.com (A. Arectout), ibtissamzidouh@gmail.com (I. Zidouh), s_younes68@hotmail.com (Y. Sadeq), azougaghma@yahoo.fr (M. Azougagh), mbouchra@hotmail.com (B. Maroufi), mahchakir@yahoo.fr (E. Chakir), hamidboukhal@gmail.com (H. Boukhal).

https://doi.org/10.1016/j.net.2021.07.028

reference conversion coefficients were calculated by several methods as described in ISO reports 4037–3 [11] and 4037–4 [12].

In this study, the X-ray Narrow-beam radiation qualities (N-60 to N-250) have been validated using both HVL and $H_p(10)$ dosimetry approaches. In addition, the X-ray spectra were also obtained using the Monte-Carlo GAMOS code [13]. In this way, the performance of GAMOS code to treat the physical processes predominant in dosimetry of X-rays was verified. A good response and low cost of the dosemeters calibration procedure are the most important advantages of this study. The X-ray beams established can be used for calibration and reference irradiation purposes. Moreover, the simulated spectra can be used in future works necessitating the explicit knowledge of the X-ray spectral distributions.

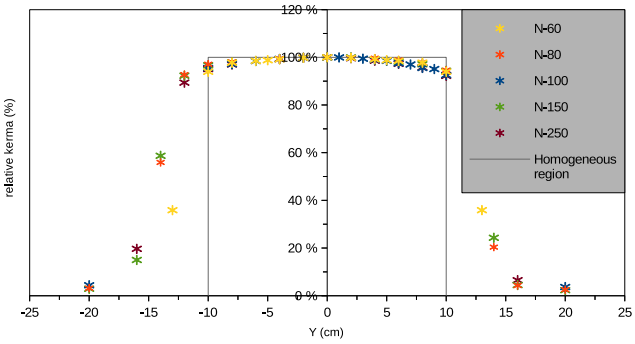

Fig. 2. Beam profile at a distance of 100 cm from the tube.

2. Experimental approach

2.1. Equipments

The measurements were performed with a Philips X-ray machine model MXR-320/26–90, which has a pure tungsten anode with an angle of 20° and inherent filtration of 3 mm of beryllium. The high voltage that can be applied to this x-ray tube varies from 10 to 320 KVp. The amount of the generated charge by the X-ray photons was measured with a spherical ionization chamber PS-50 connected to a PTW Unidos electrometer. Concerning the attenuators, aluminum and copper sheets with purity higher than 99.98% were used. The experimental set-up is shown in Fig. 1.

2.2. Beam profile

In order to ensure that the field diameter is large enough to irradiate completely the ionization chamber, measurements at different positions were carried out. These measurements were made for five qualities (N-60, N-80, N-100, N-150 and N-250) distancing 1 m from the tube focus. Fig. 2 shows the horizontal beam profiles for all these qualities. A homogeneous region with a diameter of 20 cm was obtained.

2.3. X-ray spectra characteristics

In this section, the characteristics of X-ray beam of the ISO narrow-spectrum series are presented. The X-ray beams are denoted by N-xxx, where xxx represents the high voltage (KVp) applied to the X-ray generator. The measurements were performed for five radiation qualities, namely: N-60, N-80, N-100, N-150 and N-250.

2.3.1. Determination of inherent filtration

The beam quality depends on the total filtration used during irradiation. The total filtration includes both inherent and additional filtration. The inherent filtration contributes to the absorption of the low energy portion of the x-ray beam as it passes through the X-ray tube. This absorption occurs in the material needed to provide the vacuum, electrical insulation and mechanical rigidity of the X-ray tube. The inherent filtration is usually measured using the ionization chamber placed at 1 m from the tube center. The measurement procedure consists of calculating, with 99.98% purity aluminum absorbers, the first HVL of the beam at 60 kVp tube potential and without any additional filtration. The attenuation curve in aluminum is shown in Fig. 3. The first HVL obtained from this graph was 0.425 mm Al. Therefore, the inherent filtration for our generator can be calculated by an interpolation using Table9 of ISO 4037–1 page 24 [2]. The interpolated value obtained was 0.3 mm of Al. This value was added to 3.7 mm to achieve the total filtration of 4 mm Al.

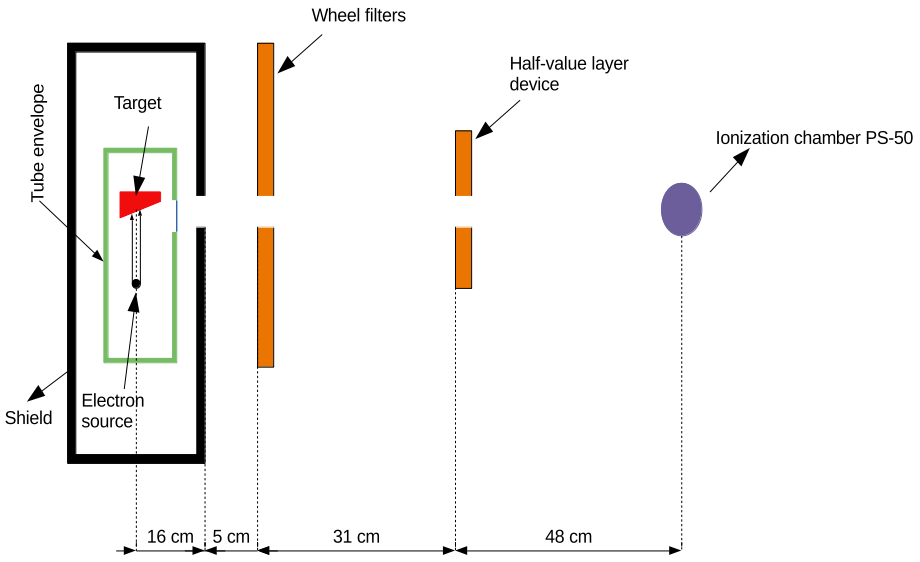

Fig. 1. Diagram of the experimental set-up.

2.3.2. HVLs measurements

The HVL measurements were performed for each radiation quality going from N-60 to N- 250. The procedure is to measure the attenuation curves using different copper filters thicknesses. The air kerma rate measurement without any filter was taken as a reference of 100% for further calculations. For each point in the attenuation curve, 10 measurements have been recorded. Using the exponential equation, it was possible to calculate the first and second half-value layers by finding the x values corresponding to 50% and 25% transmission factors respectively.

2.4. Conversion coefficients

In addition to the HVL validation, the X-ray spectra for N-60 to N-250 were validated by means of $H_p(10)$ dosimetry as specified in Paragraph 5.3 of ISO 4037–2 [10]. The ratio between the temperature and pressure corrected $H_p(10)$ dose and air kerma is calculated and compared to the ISO-specified conversion coefficients. The air kerma was measured with the ionization chamber PS-50. However, the $H_p(10)$ measurements were performed with a parallel plate ionization chamber allowing the direct measurement of personal dose equivalent on a slab phantom. Which is a secondary standard ionization detector type 34035 developed by Ankerhold et al. (1999) [14] at PTB Germany. The instrument consists of integration between a parallel plate ionization detector (measuring part) and a slab phantom (back-scattering part) made of polymethyl methacrylate (PMMA) material. The main characteristics of the $H_p(10)$ chamber are: 10 cm^3 measurement volume, dimensions of the measuring part (31 × 300 × 300 mm), and the slab phantom dimensions are 120 × 300 × 300 cm. The reference point is in the chamber center at 15.5 mm under chamber surface. The $H_p(10)$ chamber has been calibrated in the PTB laboratory for the ISO Narrow spectrum. As a result of this calibration, the value of the personal dose equivalent at a depth of 10 m for the radiation quality Q and the angle of incidence α is given by:

$$H_p(10) = N_H.k(Q,\alpha).M.k_\rho$$

Where.

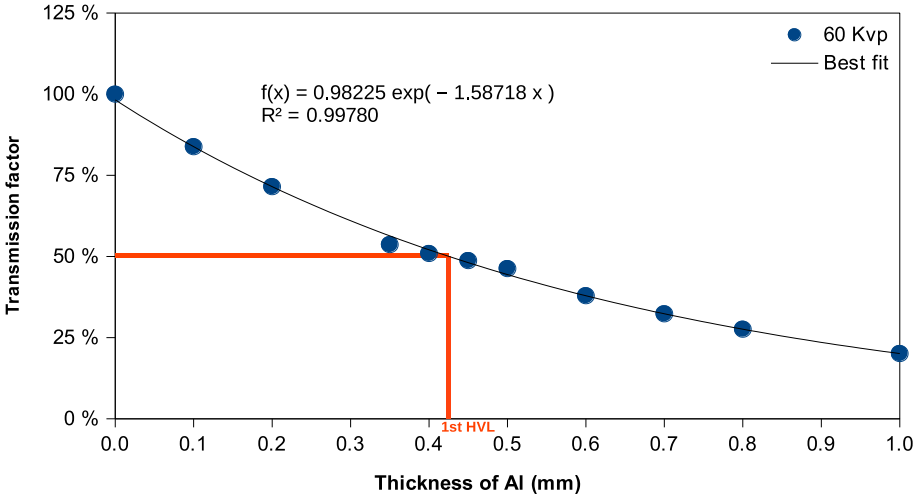

Fig. 3. HVL measurement to determine the inherent filtration.

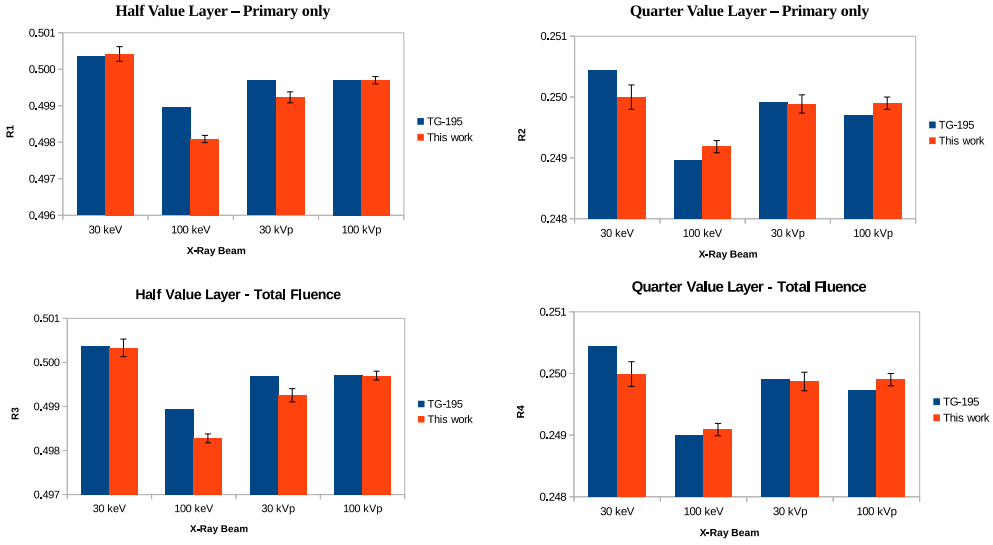

Fig. 4. Calculated values of R1, R2, R3 and R4 in Case 1. Results obtained from our MC code and that adopted in AAPM TG report 195.

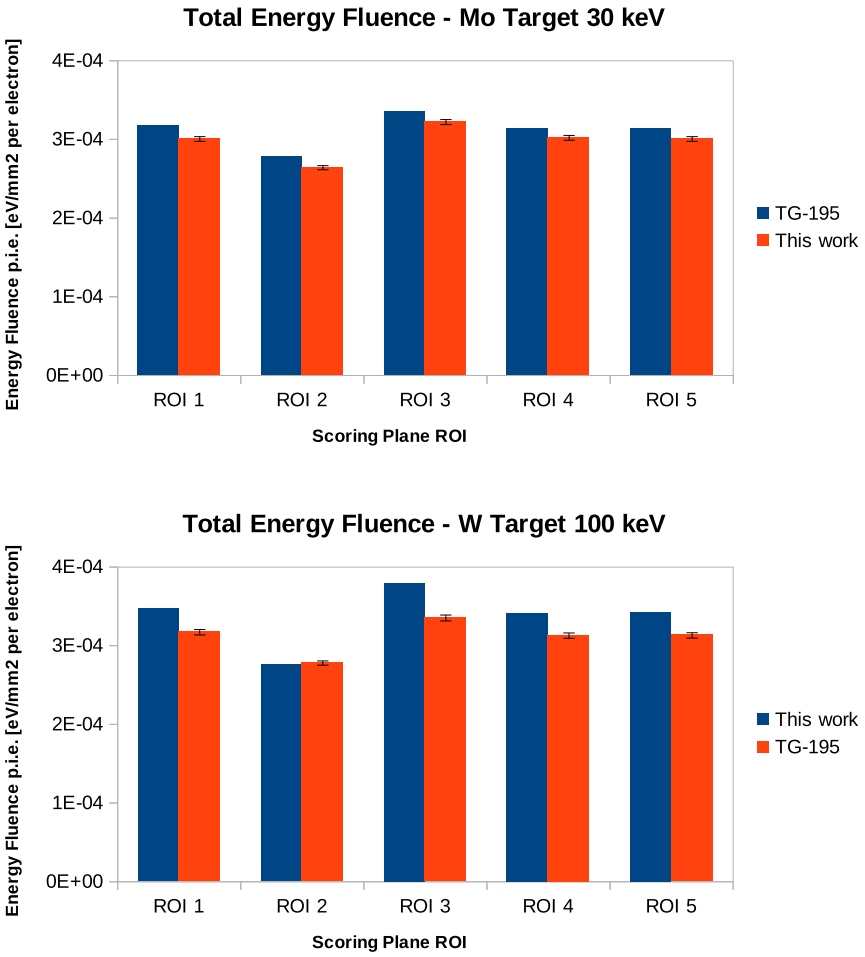

Fig. 5. Total energy fluence per initial electron at the scoring plane for the Mo target (top) and W target (bottom) simulations of x-ray production of Case 6.

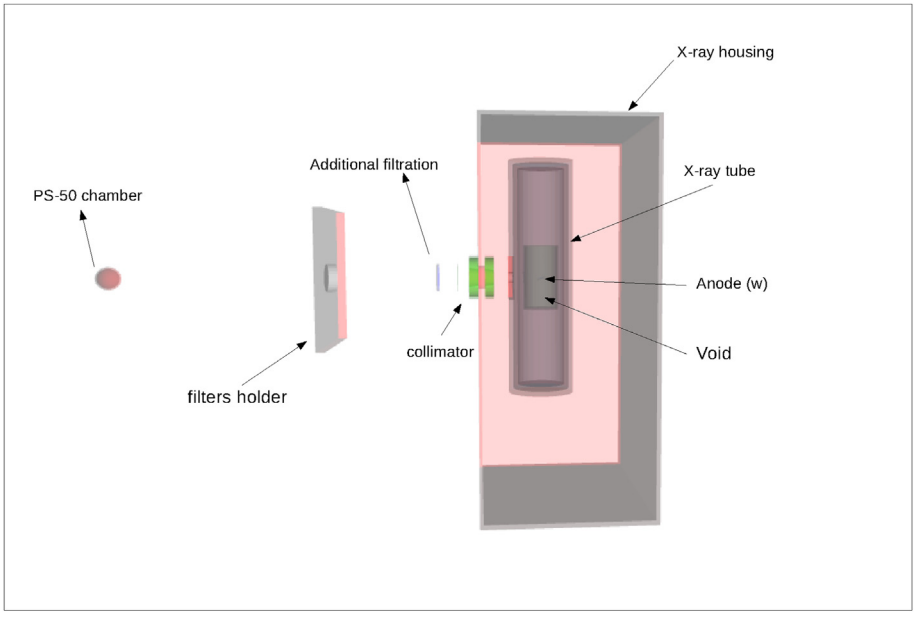

Fig. 6. Monte Carlo model of the X-ray beam irradiator set-up using VRML-X3D.

Table 1
Monte Carlo simulation parameters used in this study as recommended by AAPM TG-268.

Checklist item #	Item name	Description	References
2,3	Code, version/release date	Gamos, release 6.1.0 Feb 05, 2020	[13]
4,17	Validation	The Monte Carlo code was validated by performing the calculations of cases 1 and 6 of the American Association of Physicists in Medicine (AAPM) Task Group Report 195. Validation data are presented in section III.1.	[15]
5	Timing	Batch jobs are submitted to an HPC cluster, taking about 12 h to complete 10^9 histories.	[21]
8	Source description	The X-ray beam is modeled with a phase-space file created with the IAEA recommended format.	
9	Cross-sections	**Physics list**: GmEMPhysics **PE**: G4LivermorePhotoElectricModel **Compton**: G4LivermoreComptonModel **GC**: G4LivermoreGammaConversionModel **Rayleigh**: G4LivermoreRayleighModel **ionization**: G4LivermoreIonisationModel **bremsstrahlung**: GmLivermoreBremsstrahlungModel **multiple scattering**: G4UrbanMscModel.	[16]
10	Transport parameters	Default transport parameters, range cuts: 100 μm e−, e+ and ɤ	
11	VRT and/or AEIT	Variance reduction was performed using the Bremsstrahlung-splitting technique (BremsSplitting). The phase-space files were used with a recycle factor of 10.	
12	Scored quantities	Absorbed dose, Kerma	
13, 18	# of histories/statistical uncertainty	1×10^8-5×10^9 photons for kerma and dose calculations. Statistical uncertainty below 5% for all simulations.	
14	Statistical methods	The uncertainty for each scored quantity was calculated using the following formula: $\sqrt{\frac{\text{SumV2*nEvents} - \text{sumV}^2}{\text{nEvents} - 1} \cdot \frac{1}{\text{nEvents}}}$ where nEvents is the total number of events in the run, SumV is the sum of the scored quantity value times its weight (i.e. the scored quantity itself) and SumV2 is the sum of squares of scored quantity value times its weight.	
15, 16	Postprocessing	None	

N_H : calibration factor for the personal dose equivalent at a depth of 10 mm in unit of Sv/C.
M: dosimeter reading reduced by the background count reading in unit of C.
k_ρ: correction factor for the air density ρ in the chamber volume.
$k(Q, \alpha)$: correction factor for the radiation quality Q and the angle of incidence α.

Entering the secondary standard chamber $H_p(10)$ parameters in UNIDOS dosimeter memory, including the calibration factor NH = 3.218 × 10^6 Sv/C and uncertainty of 4% (in conformity with the corresponding calibration certificate), the dose equivalent in Sv at d = 10 mm depth is obtained.

3. Monte-Carlo simulation

3.1. Monte-Carlo code validation

The MC code was validated as suggested in the American Association of Physicists in Medicine (AAPM) report of task group 195 [15]. Cases 1 and 6 reported in the TG-195 were considered most appropriate for our application. Case 1 aims to verify the accuracy of input x-ray spectrum sampling, basic material attenuation, and HVL calculations. The validation test of this case consists of an x-ray source emitting a circular beam of 1 mm toward an aluminum filter with 40 mm diameter. The diagram of the geometry setup is shown in Fig. 2 of AAPM Report 195 (pages 11). The simulations were performed for four beams namely: 1) a monoenergetic beam at 30 keV, 2) a monoenergetic beam at 100 keV, 3) a Mo/Mo spectra at 30 kVp and 4) W/Al spectra at 100 kVp. The following quantities are calculated for each beam: R1: Half value layer for the primary fluence, R2: Quarter value layer for the primary fluence, R3: Half value layer for the total fluence (primary and scattered), and R4: Quarter value layer for the total fluence. Fig. 4 shows values of R1, R2, R3 and R4 calculated by our MC code, in comparison with TG-195 data. The results of our simulations agree to within 99% of the mean results published by TG 195 and they are within the range of results published by TG 195. It is worth noting that the highest difference obtained was 0.18% for R4 with a monoenergetic beam at 30 keV.

In addition, case 6 was examined to verify the accuracy of electron transport and x-ray generation in typical tube targets in mammography and radiography. The validation test consists of a monoenergetic electron beam with a circular area of 3 mm diameter impinged on an anode surface. The number of produced photons that traveled across the surface of a scoring area (fluence) was counted into an energy bin with 1 keV of energy width. Five scoring areas, 1 × 1 cm each, were defined for counting the fluences in different locations. The detailed geometry setup was shown in Figure 17 of AAPM Report 195 (pages 28). The X-ray spectrum was generated of two different target materials namely Mo and W anode at energy 30 keV and 100 keV respectively. The energy distribution and the integral planar energy fluence were calculated in areas 2, 1, and 3 to reflect the heel effect, and in areas 4, 1, and 5 to reflect the effect symmetry. Fig. 5 shows the results for our Monte Carlo simulation relative to this case. The results of our simulations agree to within 90% of the mean results published by TG 195 and they are within the range of results published by TG 195.

3.2. Simulation description

The simulation of X-ray production was performed using the Geant4-based Architecture for Medicine-Oriented Simulations (GAMOS) package [13]. The simulation is initiated from an accelerated electron beam hitting the anode with an angle of 22°. The energy of the electrons is determined by the X-ray tube voltage (e.g. 60 kVp corresponds to 60 keV). Each element of the X-ray tube geometry was modeled according to its technical specifications and material composition. The modeled configuration is illustrated in Fig. 6. Concerning the physics interaction models, the GmEMPhysics physics package was adopted for the parametrization of electromagnetic interactions. The GmEMPhysics physics package uses by default the Livermore low energy electromagnetic physics model for the energy range from 1 keV to about 1 GeV for both

Table 2
First and second HVLs of the N series: results from the experiment. Simulation with GAMOS. and reference values (ISO).

Quality	First HVL (mm)			Second HVL (mm)		
	Experiment	Simulation	ISO	Experiment	Simulation	ISO
N-60	0.24	0.23	0.24	0.26	0.27	0.26
N-80	0.60	0.60	0.58	0.63	0.64	0.62
N-100	1.13	1.09	1.11	1.17	1.12	1.17
N-150	2.43	2.37	2.36	2.56	2.49	2.47
N-250	5.38	5.25	5.19	5.45	5.27	5.23

electrons and gamma [16]. The low energy processes include photoelectric effect, Compton scattering, and Rayleigh scattering for gammas and ionization process, Bremsstrahlung and multiple scattering for electrons. The data used for the determination of cross-sections and for the sampling of the final state are extracted from evaluated data libraries EPDL97 [17], EEDL [18], and EADL [19].

The Uniform Bremsstrahlung Splitting (UBS) variance reduction technique was used to reduce the statistical errors of the simulation. This technique aims to increase the statistics of bremsstrahlung photons while reducing the time spent in tracking of the electrons [13]. Moreover, a phase-space file was created with the IAEA recommended format by generating a large number of electrons and collecting the x-rays reaching a plane located at 40 cm from the tube focus. The phase-space file can then be used as a virtual source of particles.

The full simulation parameters used in this work are listed in Table 1 according to the recommendations of AAPM Research Committee Task Group 268 [20].

3.3. X-ray spectra simulation

The HVLs were calculated from the attenuation curves of air kerma in copper sheets. For calculating the air kerma, GAMOS provides a GmG4PSKerma scorer class that stores, for each step in the cell, the sum of energies of the charged secondary particles produced by non-charged particles, divided by the mass of this cell. The air kerma was evaluated according to the following equation:

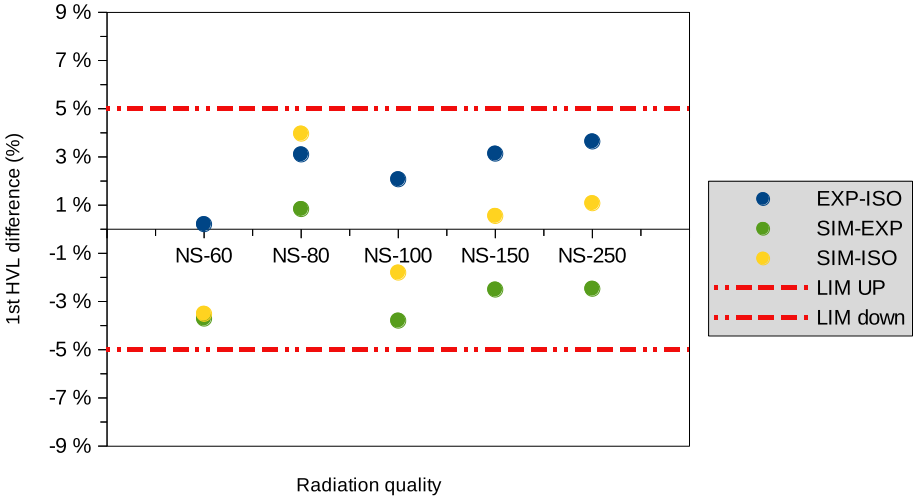

Fig. 7. Difference in 1st HVL between results obtained from the experiment, simulation and reference (ISO).

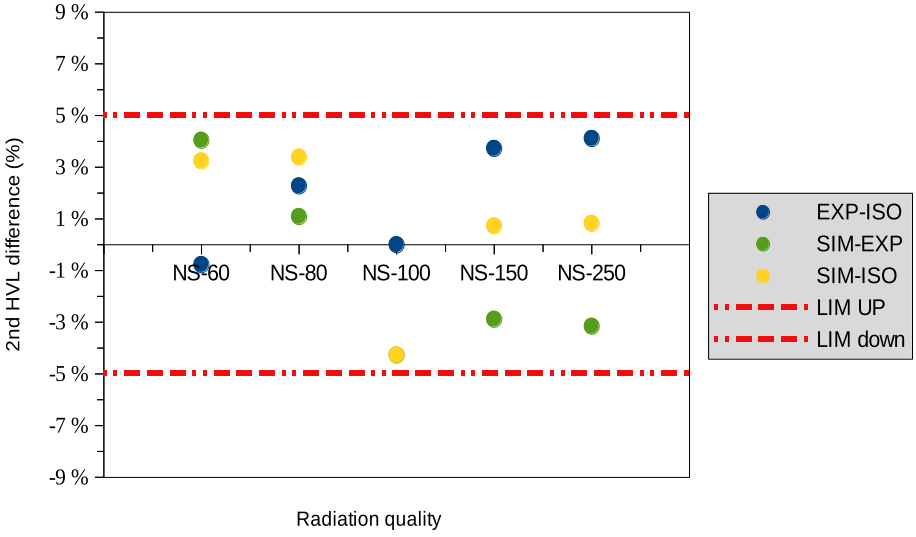

Fig. 8. Difference in 2nd HVL between results obtained from the experiment, simulation and reference (ISO).

Table 3
Mean energy and spectral resolution of narrow (N) radiation quality of simulated spectra and ISO reference.

Quality	Mean energy (keV)		Resolution (%)	
	Simulated	ISO	Simulated	ISO
N-60	48.28 ± 2.70%	48	34.84 ± 5.02%	36
N-80	65.63 ± 1.26%	65	30.79 ± 3.93%	32
N-100	81.85 ± 2.76%	83	25.94 ± 4.92%	28
N-150	117.26 ± 1.81%	118	36.32 ± 2.99%	37
N-250	204.9 ± 1.36%	208	27.94 ± 2.11%	28

$$K = \frac{\sum_{i=1}^{i=n} E_{tr}}{\rho V} \quad (1)$$

where E_{tr} is the transferred energy, n is the number of the step, ρ is the density and V the volume of the cell. This quantity is stored in a scoring volume associated with the ionization chamber. The phase-space file was used as a source of particles. The ionization chamber was modeled according to its specifications and was placed at a distance of 60 cm from the plane on which the phase-space file was created, which has a distance of 40 cm from the X-ray tube focus. The number of incident particles was chosen to produce a statistical uncertainty of less than 5% for the air kerma. In addition, the X-ray fluence spectra were simulated for each radiation quality at a distance of 1 m. The mean photon energy and the resolution spectral of the simulated spectra were calculated.

The mean photon energy is calculated by:

$$\overline{E} = \frac{\int_0^{E_{max}} \Phi_E E dE}{\int_0^{E_{max}} \Phi_E dE} \quad (2)$$

and the spectral resolution is calculated as:

$$R_E = \frac{\Delta E}{\overline{E}} \times 100 \quad (3)$$

Where ΔE is the full width at half of the fluence maximum of the spectrum andEis the mean photon energy relating to the fluence.

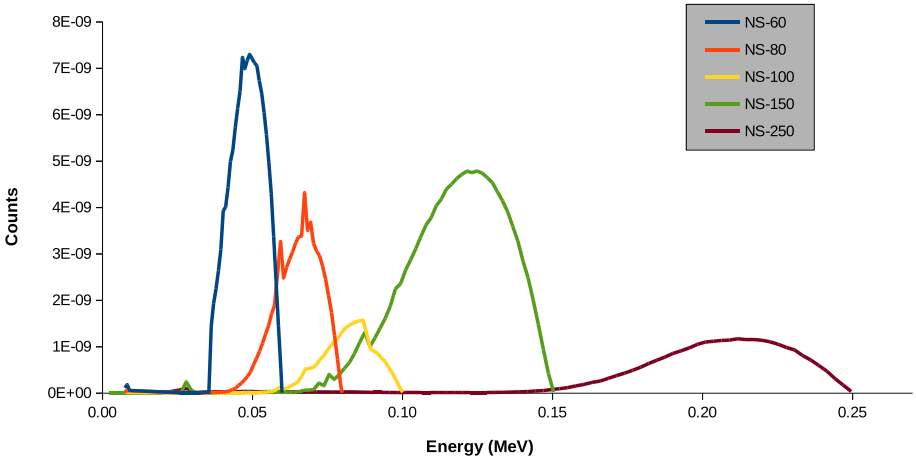

Fig. 9. X-ray spectra simulated by GAMOS.

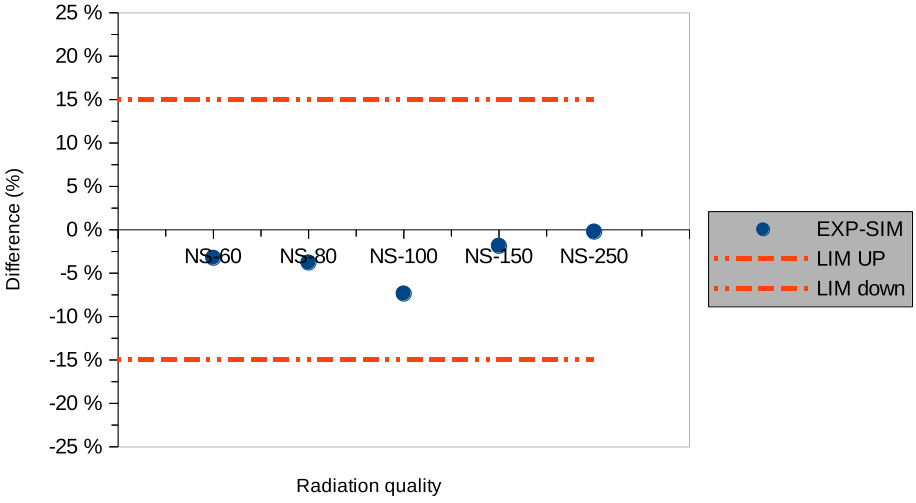

Fig. 10. Difference in spectral resolution between reference values and simulated spectra.

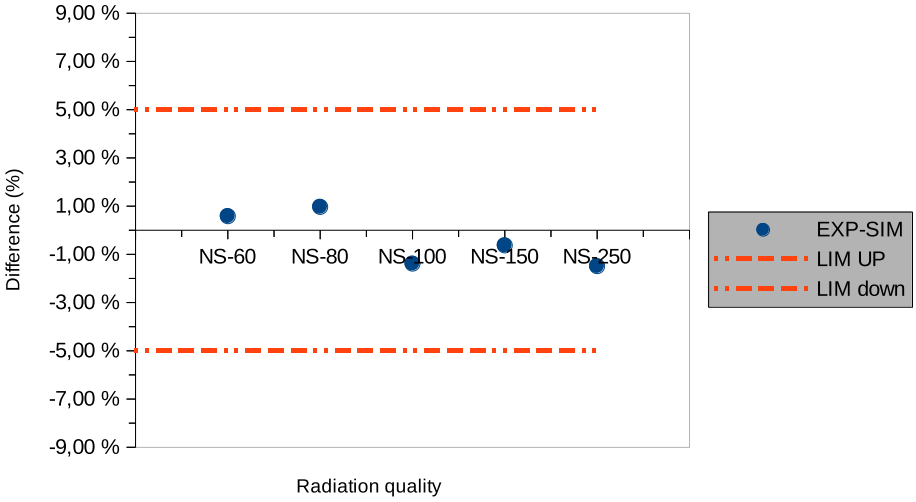

Fig. 11. Difference in mean energy between reference values and simulated spectra.

Table 4
Conversion coefficients of $h_{pk}(d)$ the ISO narrow spectra: experimental results. Simulation with GAMOS. and reference values (ISO).

Quality	Conversion coefficients $h_{pk}(10)$		
	Experiment	Simulation	ISO
N-60	1.60	1.60 ± 2.70%	1.66
N-80	1.94	1.86 ± 3.68%	1.89
N-100	1.88	1.92 ± 4.11%	1.88
N-150	1.70	1.71 ± 4.47%	1.72
N-250	1.47	1.49 ± 4.98%	1.48

3.4. Conversion coefficients

The kerma to dose equivalent conversion coefficients were calculated for the ISO water slab phantom, which is a parallelepiped made of poly-methyl methacrylate (PMMA) with an internal volume of 30 × 30 × 15 cm^3 full of water and walls of 10 mm thick except the frontal face of 2.5 mm thick. The $H_p(10)$ was evaluated by defining a scoring volume located at 10 mm from the outer surface of the phantom front wall. This volume was defined as a cylinder having a radius equal to 5 cm and a thickness of 0.01 cm. The deposited dose in the scoring volume was used to represent the $H_p(10)$ value and was obtained by using the GmG4PSDoseDeposit scorer class. Whereas the air kerma was obtained by using the GmG4PSKerma scorer class. These quantities were calculated at a distance of 1 m from the tube focus.

4. Results and discussion

4.1. X-ray spectra characteristics

The first and second half-value layers are determined for all the beam qualities of the N series, going from 60 to 250 kVp. The HVLs values obtained from the experiment and simulation were compared to the reference values (ISO). The obtained results are summarized in Table 2. According to the criterion of ISO 4037−1, *if the first and second HVLs in a given material agree within < 5% for two X-ray beams, then these two beams can be considered as equivalent.* The differences between the experimental, simulated and reference values for the first and second half value layers are shown in Figs. 7 and 8, respectively. As can be seen, the comparison in these parameters indicates a deviation inside of that allowed by the ISO. The maximum deviation between experimental and reference values of HVL_1 and HVL_2 is 3.64% and 4.11% respectively. All radiation

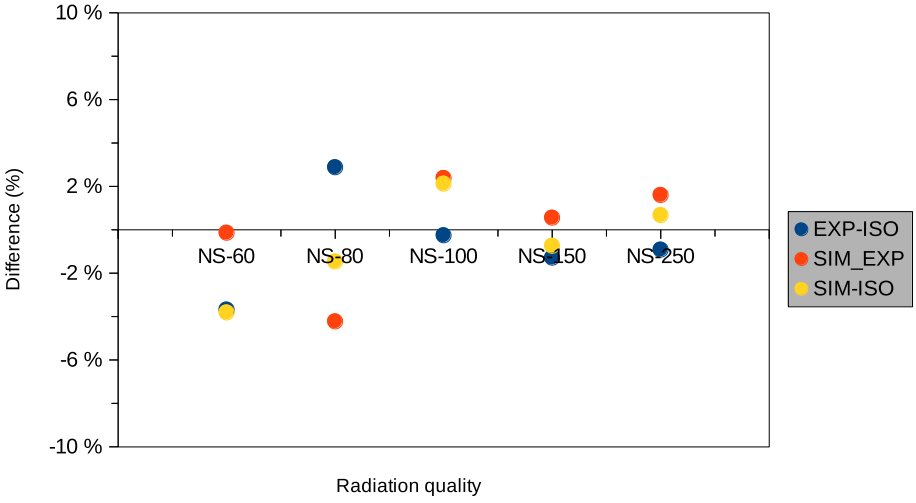

Fig. 12. Difference between conversion coefficients obtained by simulation and reference (ISO).

qualities meet the ISO criteria. Additionally, the maximum deviation between simulated and experimental values of HVL_1 and HVL_2 is 3.71% and 4.04% respectively. These results indicate that the performance of GAMOS can be considered adequate to simulate the experiment. The same comparison between the simulated and reference values indicate a deviation less than 3.97% for HVL_1 and 4.27% for HVL_2. Another comparison between the simulated spectra and the reference values was made in terms of mean photon energy and spectral resolution. This comparison was summarized in Table 3 and the simulated fluence spectra are shown in Fig. 9. The ISO 4037-1 states that *the agreement for mean energy and spectral resolution must be within < 5% and < 15%. respectively*. The difference in these parameters between the reference values and simulated results are shown in Figs. 10 and 11. All simulated spectra conform the ISO requirements. These results show that the simulated spectra are in good agreement with the reference values.

4.2. Conversion coefficients

The conversion coefficients $h_{pk}(d)$ for ISO narrow spectrum series (simulated and measured spectra) were calculated and compared with the reference values. The obtained results are summarized in Table 4. Fig. 12 shows the comparison between the experimental, simulated and reference values. The calculated conversion coefficients from measured spectra are in good agreement with the corresponding conversion coefficients obtained from the reference spectra ISO (the maximum difference is 3.68%). Additionally, one observes a reasonable agreement between the conversion coefficients obtained with the simulated spectra and those measured experimentally (the maximum difference is 4.22%). These results can be considered completely satisfactory.

5. Conclusion

In the present work, we have established some reference X-ray spectra recommended by the ISO 4037-1 standard, especially the narrow-spectrum series. The obtained results are conform to the standard values of ISO within the permissible tolerance limits of ±5% for the first and second HVLs. Furthermore, the generation of X-ray spectra has been simulated using the GAMOS Monte Carlo code. The HVLs of the simulated spectra are matching with the experimental results. They are also compatible with the standard values of ISO 4037. Moreover, the X-ray spectra produced with GAMOS present a mean energy and a resolution that agree with those of the reference radiations.

Additionally, the conversion coefficients for personal dose equivalent were calculated both experimentally and by Monte Carlo simulation. The calculated conversion coefficients for the measured spectra are in good agreement with the standard values of ISO 4037−3. The conversion coefficients for the simulated spectra present differences limited in the interval [0.14%−4.22%] compared to measured values. This is in accordance with the standard values of ISO 4037−3.

As summary, the results of this study indicate that the ISO narrow-spectrum series have been successfully established. In addition, the Monte Carlo model used to simulate the X-ray spectra is valid and can be used in works requiring knowledge of the X-ray spectral distributions.

Declaration of competing interest

The authors declare that they have no known competing financial interests or personal relationships that could have appeared to influence the work reported in this paper.

Acknowledgment

This research was supported through computational resources of HPC-MARWAN (www.marwan.ma/hpc) provided by the National Center for Scientific and Technical Research (CNRST), Rabat, Morocco.

References

[1] International Atomic Energy Agency, International Basic Safety Standards for Protection against Ionizing Radiation and for the Safety of Radiation Sources. IAEA Safety Series, vol. 115, 1996 (Vienna: IAEA).
[2] International Organization for Standardization: 'X and Gamma Reference Radiation for Calibrating Dosemeters and Doserate Meters and for Determining Their Response as a Function of Photon Energy Part1: Radiation Characteristics and Production Methods', ISO 4037-1:2017.
[3] M. Moralles, D.A.B. Bonifácio, M. Bottaro, M.A.G. Pereira, Monte Carlo and Least-Squares Methods Applied in Unfolding of X-Ray Spectra Measured with Cadmium Telluride Detectors, vol. 580, 2007, pp. 270–273.
[4] D. Kurková, L. Judas, X-ray tube spectra measurement and correction using a CdTe detector and an analytic response matrix for photon energies up to 160 keV, Radiat. Meas. 85 (2016) 64–72.
[5] M.R. Ay, M. Shahriari, S. Sarkar, M. Adib, H. Zaidi, Monte Carlo simulation of X-ray spectra in diagnostic radiology and mammography using MCNP4C, Phys. Med. Biol. 49 (2004) 4897.
[6] C.C. Guimaraes, M. Moralles, E. Okuno, Performance of GEANT4 in dosimetry applications: calculation of X-ray spectra and kerma-to-dose equivalent conversion coefficients, Radiat. Meas. 43 (2008) 1525–1531.
[7] R. Taleei, M. Shahriari, Monte Carlo simulation of X-ray spectra and evaluation of filter effect using MCNP4C and FLUKA code, Appl. Radiat. Isot. 67 (2009) 266–271.
[8] A. Herrati, M. Arib, T. Sidahmed, K. Khalal-Kouache, Establishment of ISO 4037-1 X-ray narrow-spectrum series at SSDL of Algiers, Radiat.Prot.Dosim. 174 (2016) 35–52.
[9] D. Zhang, W. Lai, J. Wu, H. Du, R. Zhao, S. Fan, Establishment of ISO 4037-1 X-ray narrow-spectrum series, J. Eng. 23 (2019) 8858–8861.
[10] International Organization for Standardization: 'X and Gamma Reference Radiation for Calibrating Dosemeters and Doserate Meters and for Determining Their Response as a Function of Photon Energy Part 2: Dosimetry for Radiation Protection over the Energy Ranges from 8 keV to 1,3 MeV and 4 MeV to 9 MeV', ISO 4037-2: 2017.
[11] International Organization for Standardization: 'X and Gamma Reference Radiation for Calibrating Dosemeters and Doserate Meters and for Determining Their Response as a Function of Photon Energy — Part 4: Calibration of Area and Personal Dosemeters in Low Energy X Reference Radiation Fields', ISO 4037-3:2017.
[12] International Organization for Standardization: 'X and gamma reference radiation for calibrating dosemeters and doserate meters and for determining their response as a function of photon energy — Part 4: calibration of area and personal dosemeters in low energy X reference radiation fields', ISO 4037-4: 2017.
[13] P. Arce, P. Rato, M. Canadas, I.J. Lagares, GAMOS: A Geant4-based easy and flexible framework for nuclear medicine applications, in: IEEE Nuclear Science Symposium Conference Record, 2008, pp. 3162–3168.
[14] U. Ankerhold, R. Behrens, P. Ambrosi, A prototype ionisation chamber as a secondary standard for the measurement of personal dose equivalent, Hp (10), on a slab phantom, metry. Radiation protection dosi 86 (1999) 167–173.
[15] I. Sechopoulos, E.S. Ali, A. Badal, A. Badano, J.M. Boone, I.S. Kyprianou, A.C. Turner, Monte Carlo reference data sets for imaging research: executive summary of the report of AAPM Research Committee Task Group 195, Med. Phys. 42 (10) (2015) 5679–5691.
[16] G.E.A.N.T. Collaboration, Physics reference manual, Versiones: geant4 9 (2016), 0.
[17] D.E. Cullen, J.H. Hubbell, L. Kissel, EPDL97: the Evaluated Photo Data Library97 Version (No. UCRL-50400-Vol. 6-Rev. 5), Lawrence Livermore National Lab., CA (United States), 1997.
[18] S.T. Perkins, D.E. Cullen, S.M. Seltzer, Tables and graphs of electron-interaction cross-sections from 10 eV to 100 GeV derived from the LLNL evaluated electron data library (EEDL), Z= 1-100, UCRL-50400 31 (1991) 21–24.
[19] S.T. Perkins, D.E. Cullen, M.H. Chen, J. Rathkopf, J. Scofield, J.H. Hubbell, Tables and Graphs of Atomic Subshell and Relaxation Data Derived from the LLNL Evaluated Atomic Data Library (EADL), Z= 1–100 (No. UCRL-50400-Vol. 30), Lawrence Livermore National Lab., CA (United States), 1991.
[20] I. Sechopoulos, D.W. Rogers, M. Bazalova-Carter, W.E. Bolch, E.C. Heath, M.F. McNitt-Gray, J.F. Williamson, RECORDS: improved reporting of Monte Carlo RaDiation transport studies: report of the AAPM Research Committee Task Group 268, Med. Phys. 45 (1) (2018) e1–e5.
[21] HPC-Marwan, URL, https://www.marwan.ma/index.php/services/hpc.